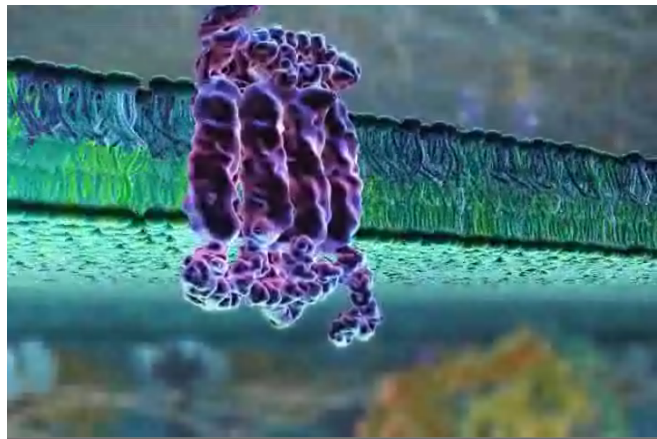
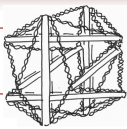


## 5.1 biomembranes - motivation



the inner life of a cell, viel & iue, harvard [2006]

## me239 mechanics of the cell

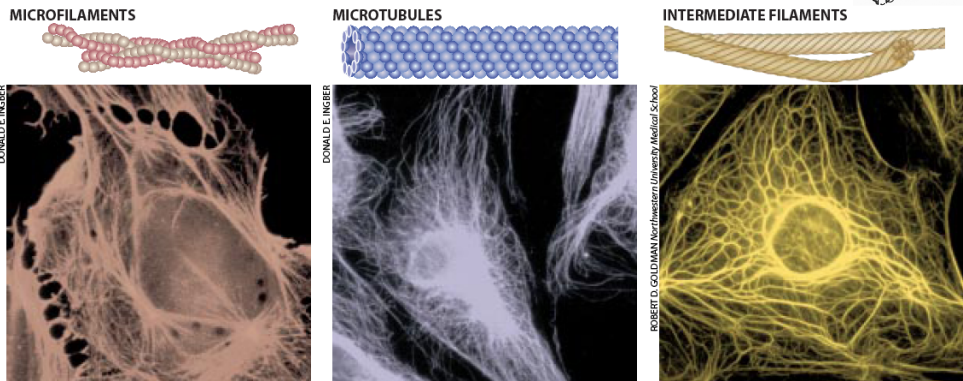
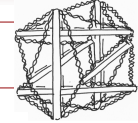


tensegrity = tension + integrity

the term tensegrity was first coined by buckminster fuller to describe a structure in which **continuous tension** in its members forms the **basis for structural integrity**. fuller most famously demonstrated the concept of tensegrity in architecture through the **design of geodesic domes** while his student, the artist kenneth snelson, applied the concept of tensegrity to creating sculptures that appear to defy gravity. snelson's tensegrity sculptures are minimal in components and achieve their stability through dynamic distribution of tension and compression forces amongst their members to create internal balance. it was upon viewing snelson's art that donald ingber became inspired by the sculpture's structural efficiency and dynamic force balance to **adopt tensegrity as a paradigm** upon which to **analyze cell structure** and mechanics. it has been 30 years since the premier appearance of the cellular tensegrity model. although the model is still largely under discussion, empirical evidence suggests that the model may explain a wide variety of phenomena ranging from tumor growth to cell motility.

## 4.4 tensegrity model for cells

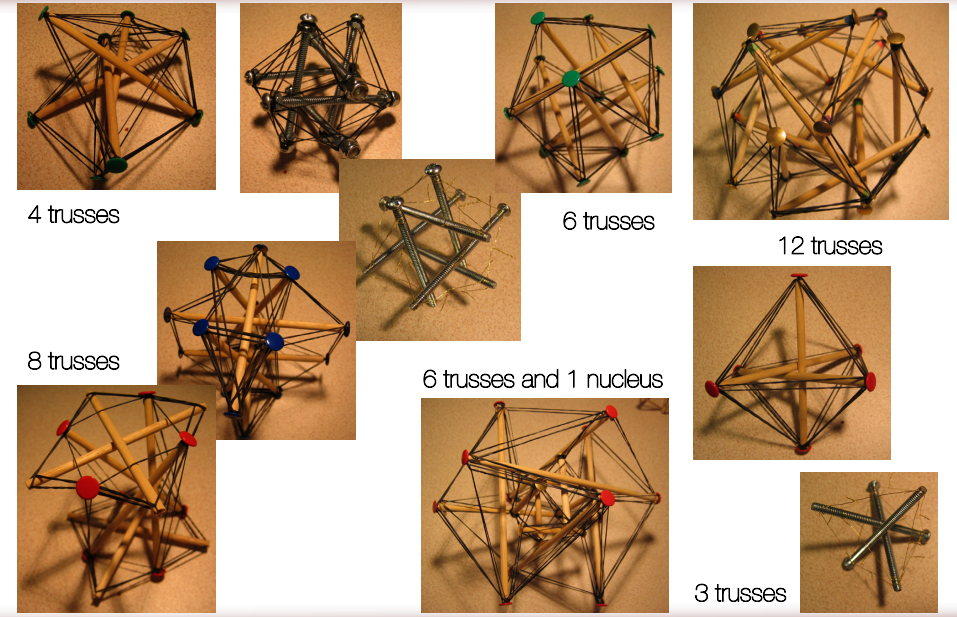
tensegrity = tension + integrity



balanced interplay between tension and compression

ingber [1998]

## 4.4 tensegrity model for cells



3

## 4.4 tensegrity model for cells

4



## network kinematics

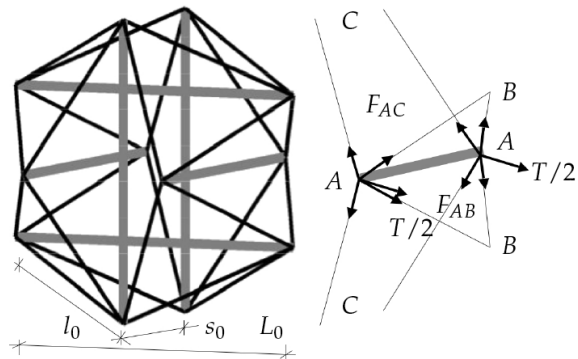
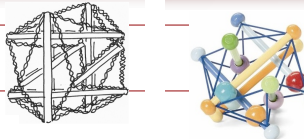
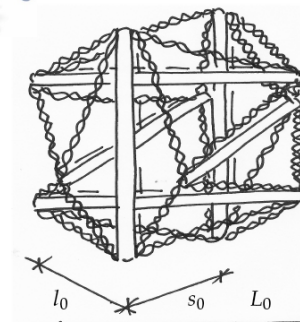


**Figure 4.12:** Kinematics of simple tensegrity cell model consisting of six compressive trusses (grey) and 24 tensile ropes (black). In the original state, all trusses are of the same length  $L_0$ , the rope lengths are  $l_0 = \sqrt{3/8} L_0$ , and the distances between two parallel trusses are  $s_0 = 1/2 L_0$ .



## tensegrity models for cells



$E_0$  ... incremental modulus  
 $F_0$  ... resting force in actin filaments  
 $L_0$  ... length of microtubules  
 $l_0$  ... resting length of actin filaments  
 $\varepsilon_0$  ... strain in actin filaments

$$W^{\text{mac}} \doteq W^{\text{mic}}$$

$$E = \frac{2\sqrt{3}}{5\sqrt{2}l_0} \frac{T}{s_x - s_0}$$

$$W^{\text{mac}} = \frac{1}{2} \varepsilon E \varepsilon$$

$$W^{\text{mic}} = \frac{1}{V_0} \int_{s_0}^{s_x} T dx$$

small strain

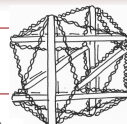
$$E_0 = 5.85 \frac{F_0}{l_0^2} \frac{1 + 4\varepsilon_0}{1 + 12\varepsilon_0}$$


---

## 4.4 tensegrity model for cells

5

### prestress - analytically predicted



- assume prestress is approximately equal in all three directions

$$P \approx \frac{1}{3} \nu^{\text{actin}} \sigma^{\text{actin}}$$

- volume fraction of actin filaments

$$\nu^{\text{actin}} = \frac{V^{\text{actin}}}{V_0} = \frac{24A^{\text{actin}}l_0}{[5\sqrt{2}]/[3\sqrt{3}]l_0^3} = \frac{24A^{\text{actin}}}{1.3608l_0^2}$$

- stress in a typical actin filament

$$\sigma^{\text{actin}} = \frac{F_0}{A^{\text{actin}}}$$

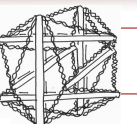
- approximation of prestress

$$P \approx \frac{1}{3} \nu^{\text{actin}} \sigma^{\text{actin}} = \frac{1}{3} \frac{24 A^{\text{actin}}}{1.3608l_0^2} \frac{F_0}{A^{\text{actin}}} \quad P \approx 5.85 \frac{F_0}{l_0^2} = E$$

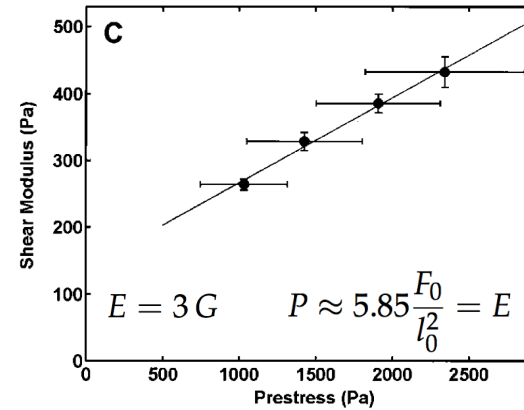
prestress is of the same order as young's modulus

6

## 4.4 tensegrity model for cells



### prestress - experimentally measured



prestress is of the same order as young's modulus

wang, naruse, stamenovic, fredberg, mijailovich, tolle-norrellykke, polte, manni, ingber [2001]

## 4.4 tensegrity model for cells

7

## 4.4 tensegrity model for cells

8

## the cell membrane



all cellular components are contained within a cell membrane which is **extremely thin**, approximately 4-5nm, and **very flexible**. Inside the cell membrane, most cells behave like a liquid as they consist of more than 50% of water. The cell membrane is **semi-permeable** allowing for a controlled exchange between intracellular and extracellular components and information.

### mechanisms of transport through the membrane

- passive transport driven by gradients in concentration
- active transport that does require extra energy; it is regulated by ion channels, pumps, transporters, exchangers and receptors

## the cell membrane



The barrier between the inner and outer cell is the cell membrane, a **bilayer** consisting of **phospholipids** of a characteristic structural arrangement. In aqueous solutions, these phospholipids essentially display two kinds of non-covalent interactions.

### non-covalent interactions of phospholipids

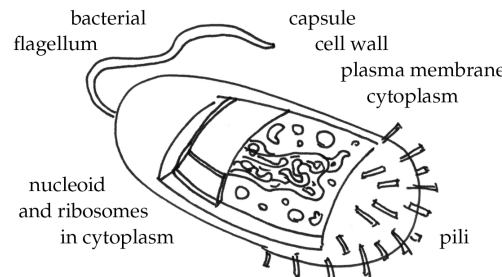
- hydrophobic, water avoiding non-polar residues
- hydrophilic, water loving polar head groups

This behavior is similar to fatty acids or **oil in water**, where the hydrophilic polar heads tend to be oriented towards the water phase while the hydrophobic tails are oriented towards the oil phase.

## 5.1 biomembranes - motivation

9

### the cell wall



In most cells, the **internal pressure** is much higher than the surrounding pressure. The cell membrane thus has to be strong enough to **prevent the explosion** of the cell. Plant cells and most bacteria have found an efficient solution to withstand the internal pressure: their cells have an **external wall** to reinforce their cell membrane and balance the pressure difference across it.

## 5.1 biomembranes - motivation

11

## 5.1 biomembranes - motivation

10

### the lipid bilayer

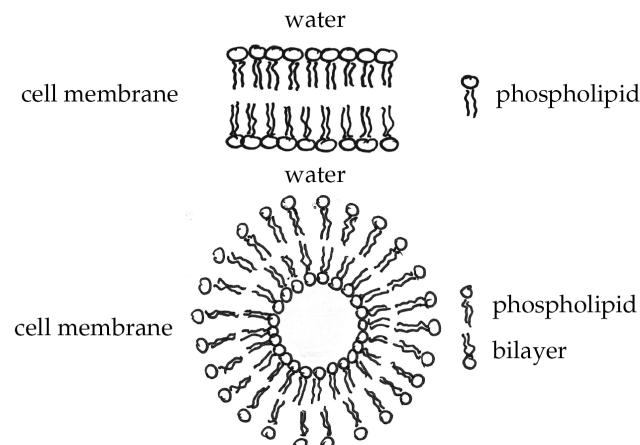
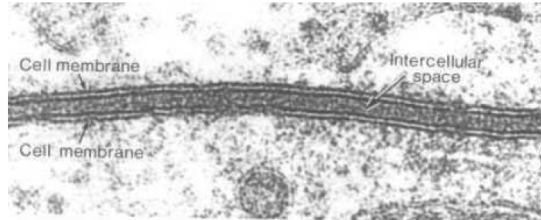


Figure 5.16. Lipid bilayer of the cell membrane. Characteristic arrangement of phospholipid molecules with hydrophilic polar head group being oriented towards the aqueous phase while the hydrophobic tails are oriented towards the non-polar inside.

## 5.1 biomembranes - motivation

12

## the lipid bilayer



**Figure 5.1:** Electron microscopy of the cell membrane stained with osmium tetroxide illustrating the polar head groups with a light 2nm space of hydrophobic tails sandwiched between them, adopted from [4]

## the cell membrane

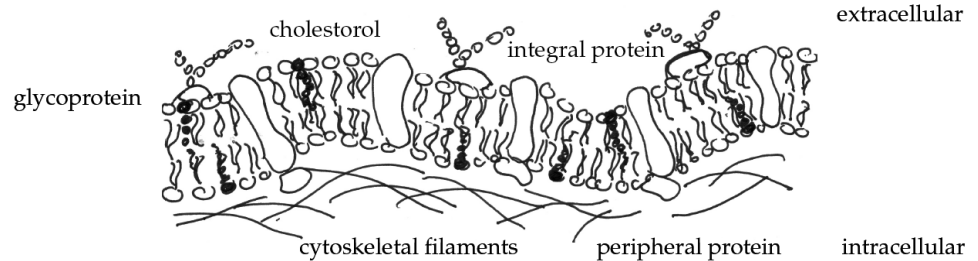


**Figure 1.3.** Cell membrane. Phospholipid bilayer with hydrophobic water-avoiding tails and hydrophilic water-loving heads.

## 5.1 biomembranes - motivation

13

## the lipid bilayer

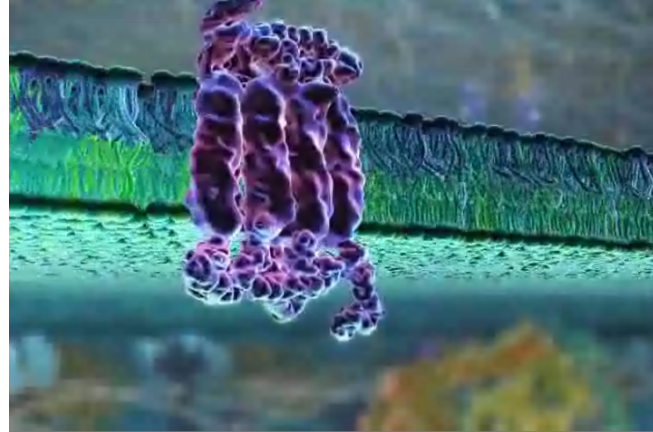


**Figure 1.5.1.** Lipid bilayer of the cell membrane. Characteristic arrangement of phospholipid molecules with hydrophilic polar head group being oriented towards the aqueous phase while the hydrophilic tails are oriented towards the non-polar inside.

the inner life of a cell, viel & lue, harvard [2006]

## 5.1 biomembranes - motivation

15

## 5.1 biomembranes - motivation

14

## the lipid bilayer - lipid rafts

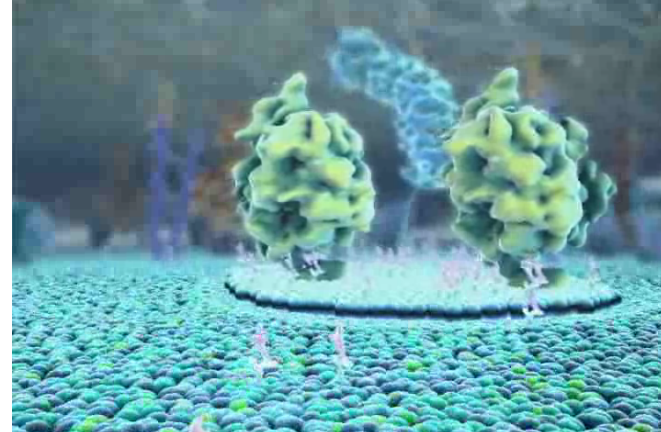


**Figure 1.5.2.** The lipid bilayer of the cell membrane is by no means static and homogeneous. Lipids are a class of molecules stacking together to form the membrane which can be understood as a sea on which things are floating. The rafts floating on this sea are called lipid rafts.

the inner life of a cell, viel & lue, harvard [2006]

## 5.1 biomembranes - motivation

16

## micropipette aspiration

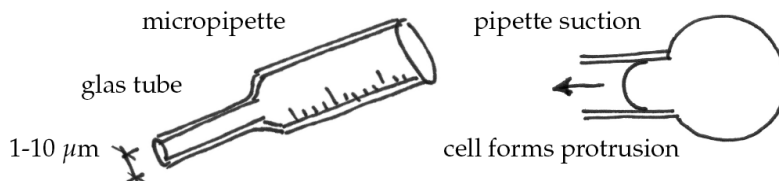


**Figure 5.2:** During micropipette aspiration, a cell is aspirated into a thin glass tube. Knowing the applied suction pressure, we can determine the surface tension of the cell based on changes in cell geometry.

## micropipette aspiration

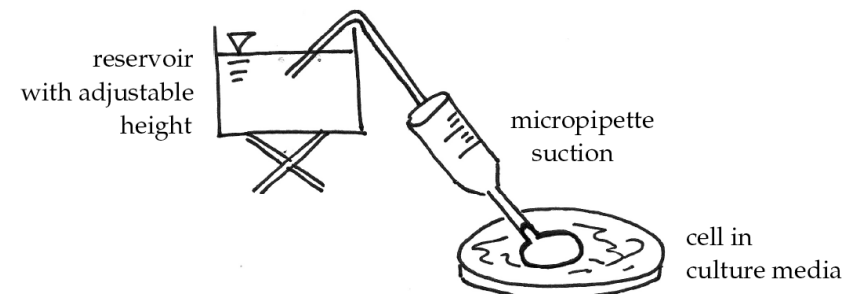


**Figure 5.3:** Experimental setup of micropipette aspiration. The applied suction pressure can be varied by adjusting the height of a fluid filled reservoir. Cell deformation is measured optically.

### 5.1.1 micropipette aspiration

17

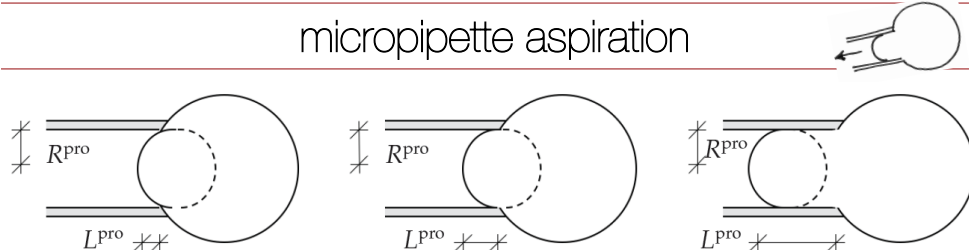


**Figure 5.4:** The three stages during micropipette aspiration. The initial state with  $L^{\text{pro}} / R^{\text{pro}} < 1$ , left, the critical state with  $L^{\text{pro}} / R^{\text{pro}} = 1$ , middle, and the final state with  $L^{\text{pro}} / R^{\text{pro}} > 1$ , right.

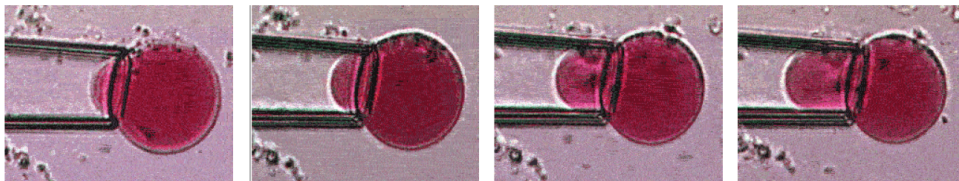


**Figure 5.5:** Experimental observation of different stages during micropipette aspiration adopted from <http://newton.ex.ac.uk/research/biomedical/membranes>.

### 5.1.1 micropipette aspiration

19

### 5.1.1 micropipette aspiration

18

## surface tension

$$n = \sigma h \quad \text{with} \quad [n] = [\text{force} / \text{length}]$$

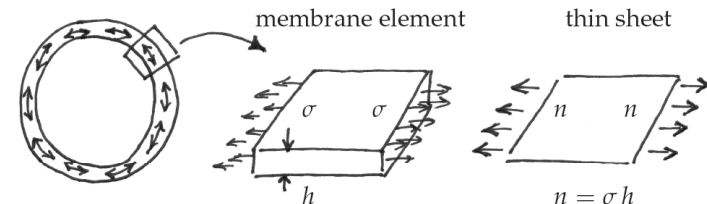
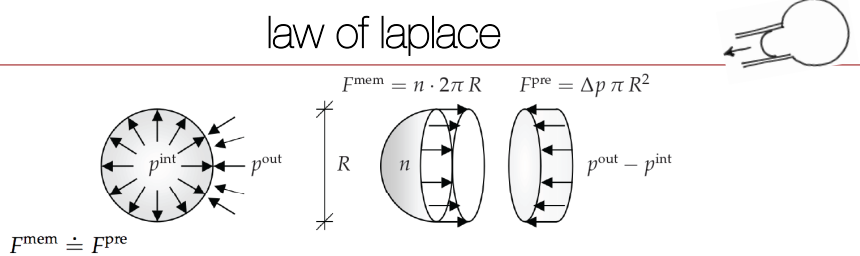


**Figure 5.6:** Liquid drop model. The internal fluid pressure is balanced by a thin elastic shell. The membrane element of thickness  $h$  is subjected to membrane stresses  $\sigma$ . Equivalently, the membrane can be represented as a thin sheet subjected to the surface tension  $n$  which results from the integration of the membrane stress over the thickness as  $n = \sigma h$ .

### 5.1.1 micropipette aspiration

20



where

$$F^{\text{mem}} = n C \quad \text{with} \quad C = 2\pi R$$

are the forces of the cell membrane acting along the circumference  $C$  and

$$F^{\text{pre}} = [p^{\text{int}} - p^{\text{out}}] A \quad \text{with} \quad A = \pi R^2$$

are the forces generated by the pressure difference across the cell wall acting on the surface area  $A$ . When combining these three equations, we obtain the law of Laplace

$$p^{\text{int}} - p^{\text{out}} = 2 \frac{n}{R} \quad \dots \text{Law of Laplace}$$

## 5.1.1 micropipette aspiration

21

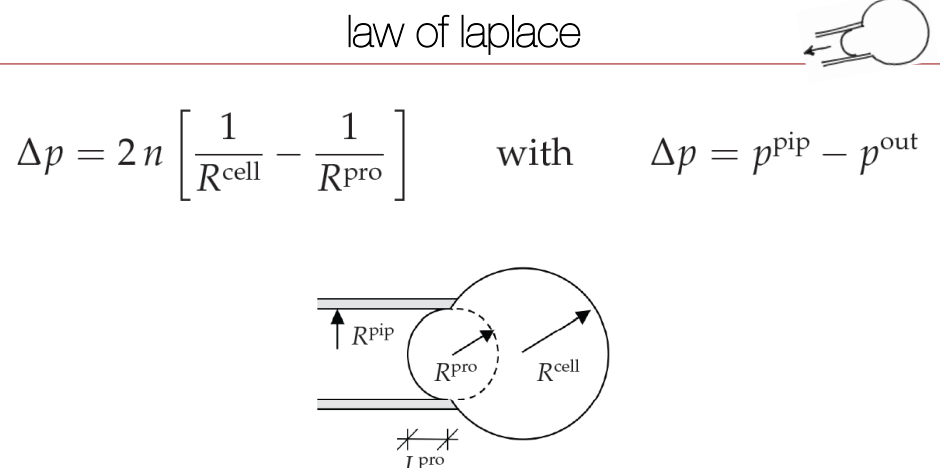


**Figure 5.8:** Kinematics of micropipette aspiration. For the limit state, at  $L^{\text{pro}}/R^{\text{pro}} = 1$ , the Law of Laplace can be used to determine the surface tension  $n$ .

## 5.1.1 micropipette aspiration

23

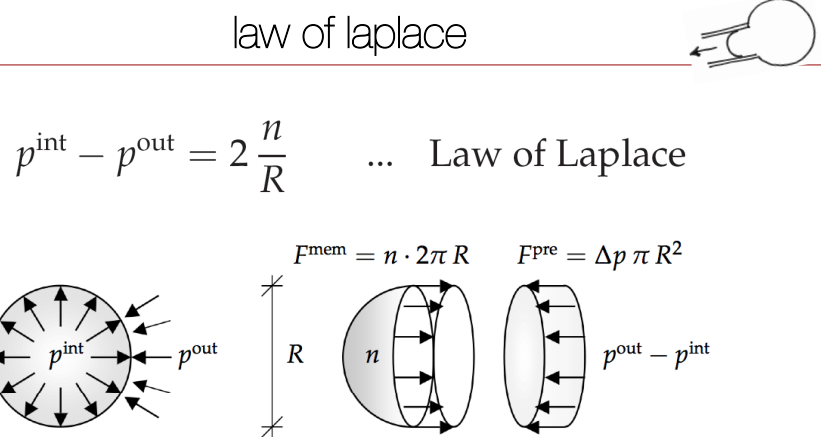


**Figure 5.7:** Law of Laplace. The membrane force  $F^{\text{mem}} = n \cdot 2\pi R$  is the result of the surface tension  $n$  acting on the cell membrane along the circumference  $C = 2\pi R$ . It is in equilibrium with the forces  $F^{\text{pre}}$  resulting from the pressure difference  $\Delta p$  acting on the cell area  $A = \pi R^2$ .

## 5.1.1 micropipette aspiration

22

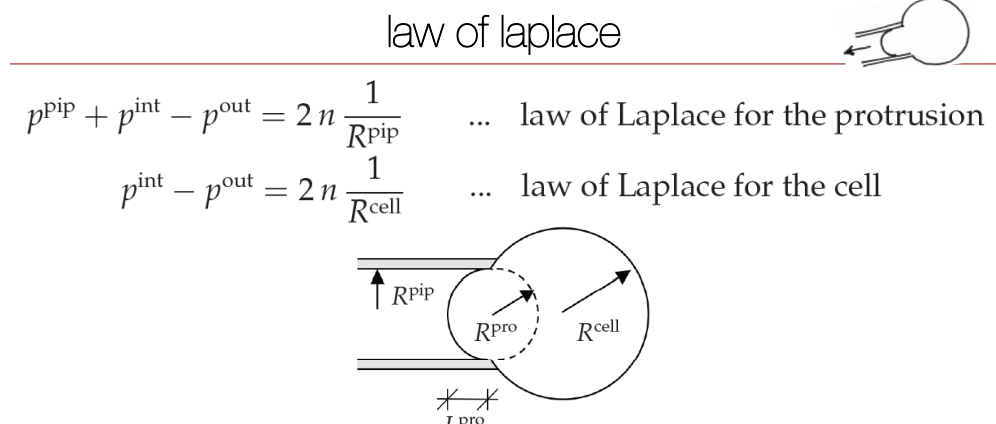


**Figure 5.8:** Kinematics of micropipette aspiration. For the limit state, at  $L^{\text{pro}}/R^{\text{pro}} = 1$ , the Law of Laplace can be used to determine the surface tension  $n$ .

$$p^{\text{pip}} = 2n \left[ \frac{1}{R^{\text{pip}}} - \frac{1}{R^{\text{cell}}} \right]$$

## 5.1.1 micropipette aspiration

24

## micropipette aspiration

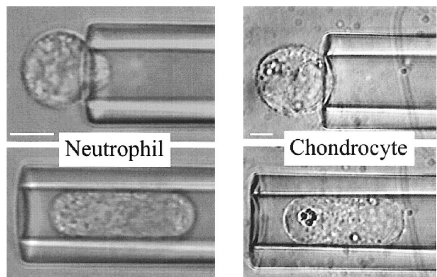


Fig. 4. A neutrophil and a chondrocyte each being aspirated into a micropipette. The photomicrographs of the chondrocyte are adapted from Jones et al. (1999). The scale bars indicate 5  $\mu\text{m}$ .

**summary** neutrophils behave as liquid drops with a cortical surface tension of about 30 pN/ $\mu\text{m}$  and a viscosity of the order of 100 Pa, chondrocytes and endothelial cells behave as solids with an elastic modulus of the order of 500 pN/ $\mu\text{m}$ =0.5 kPa.

hochmuth [2000]

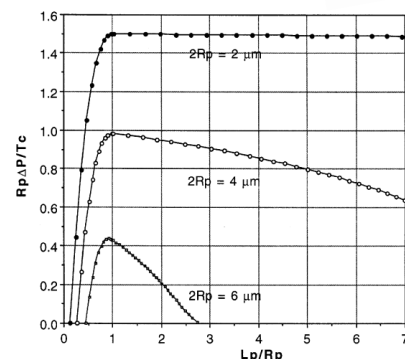


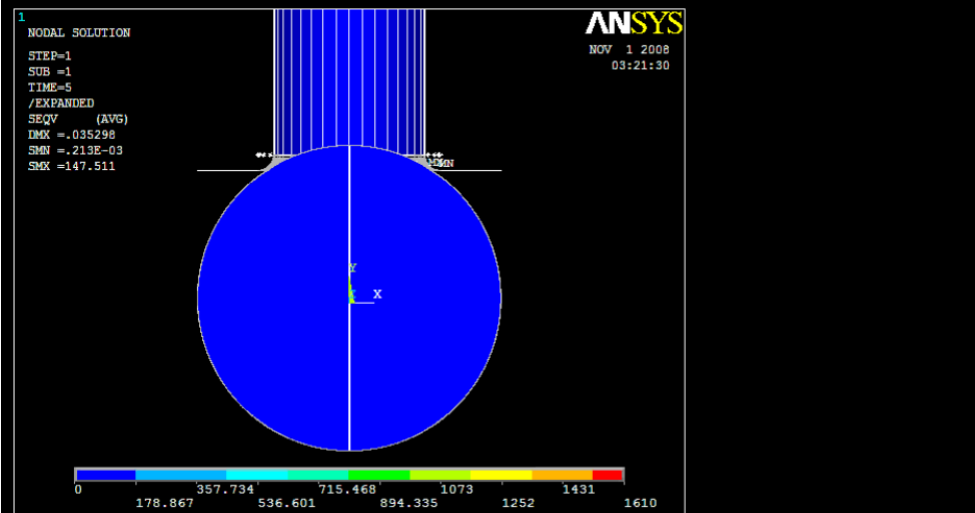
Fig. 5. The aspiration into a pipette of a liquid drop with a constant cortical surface tension  $T_c$  according to (3).  $L_p$  is the length of extension of the drop into the pipette, and  $R_p$  is the radius of the pipette. When  $L_p/R_p > 1$ , the results are no longer stable to an increase in pressure. Thus, the cell flows freely into the pipette when the pressure is increased beyond the point where  $L_p/R_p = 1$ . Cells such as neutrophils that flow freely into pipettes at this point behave as liquid drops.

## 5.1.1 micropipette aspiration

25

zubin huang [2007]

## finite element simulation of micropipette aspiration



## 5.1.1 micropipette aspiration

27

## finite element simulation of micropipette aspiration

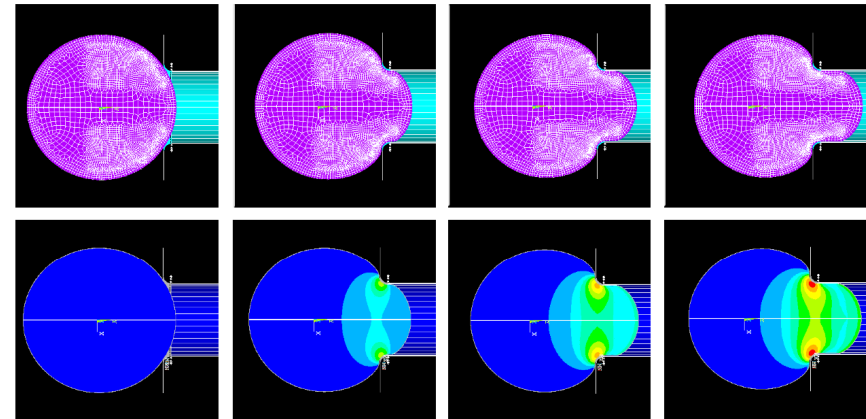


Figure 5.10: Finite element simulation of micropipette aspiration of a chondrocyte modeled as an elastic solid. In contrast to analytical results, finite element simulations can account for large deformations, heterogeneous stress distributions, and a more realistic representation of the boundary conditions [21].

## 5.1.1 micropipette aspiration

26

prashant purohit, university of pennsylvania

## heterogeneous fluctuating rod models for unfolded proteins and application to fibrin networks

biofilaments, such as, actin and DNA, have for long been modeled as thermally fluctuating elastic rods with homogeneous material properties. such models are adequate if the length scale of the filaments being studied is much larger than the scale of the heterogeneity. however, advanced single molecule experimental techniques have now made it possible to probe the properties of biomolecules at the scale of a few nanometers. the data emerging from these experiments ought to be greeted with appropriately detailed models. in this presentation we study the mechanics of a thermally fluctuating elastic rod whose moduli are a function of position. such a rod can be used as a model for DNA whose sequence specific properties are known or for a protein oligomer in an AFM where some of the monomers might be unfolded. the mechanics of these rods is understood by first evaluating a partition function through path integral techniques. similar methods can also be applied to heterogeneous networks of filaments. in this presentation we will show how protein unfolding at the level of a single filament can determine the macroscopic mechanical behavior of a network.

mechanics & computation, me395, thu 02/03/11, 4:15-5:25, 320-105

## heterogeneous fluctuating rod models

28